

Random walker in temporally deforming higher-order potential forces observed in a financial crisis

Kota Watanabe,^{1,*} Hideki Takayasu,² and Misako Takayasu¹

¹*Department of Computational Intelligence & Systems Science, Interdisciplinary Graduate School of Science & Engineering, Tokyo Institute of Technology, 4259-G3-52 Nagatsuta-cho, Midori-ku, Yokohama 226-8502, Japan*

²*Sony Computer Science Laboratories Inc., 3-14-13 Higashigotanda, Shinagawa-ku, Tokyo 141-0022, Japan*

(Received 27 November 2008; revised manuscript received 16 August 2009; published 19 November 2009)

Basic peculiarities of market price fluctuations are known to be well described by a recently developed random-walk model in a temporally deforming quadratic potential force whose center is given by a moving average of past price traces [M. Takayasu, T. Mizuno, and H. Takayasu, *Physica A* **370**, 91 (2006)]. By analyzing high-frequency financial time series of exceptional events, such as bubbles and crashes, we confirm the appearance of higher-order potential force in the markets. We show statistical significance of its existence by applying the information criterion. This time series analysis is expected to be applied widely for detecting a nonstationary symptom in random phenomena.

DOI: [10.1103/PhysRevE.80.056110](https://doi.org/10.1103/PhysRevE.80.056110)

PACS number(s): 89.65.Gh, 02.50.Ey, 05.45.Tp

I. INTRODUCTION

Financial bubbles and crashes have been occurring occasionally in nearly every market causing social troubles of various magnitudes. In the normal market state, prices fluctuate fairly randomly and directional prediction is almost impossible; however, during bubbles and crashes, the market prices are known to move quite asymmetrically [1]. Viewing the movement of prices in a coarse-grained way reveals that the growth of price in a bubble period is approximated either by an exponential function [2,3], a double-exponential function [4], or a function having a finite-time singularity [5–10]. In any case, it is a reasonable assumption that there are some special mechanisms of bubbles that are quite different from the normal market state. It is very important to develop the technique to quantify the financial risk of large price changes [11].

In the year 1900, Bachelier introduced the first random-walk model as a model of market price fluctuations [12]. The stochastic model based on his mathematical theory was developed in the field of financial technology and it is widely accepted in the real financial market.

In the 1990s, analysis of high-frequency tick-by-tick data by physicist clarified that market price is not a simple random walk [13]. The market price has some empirically stylized facts, which clearly deviate from a pure random walk. In order to build a model, which fulfills those properties, many variants of random-walk models of market prices have been proposed.

Recently, one of the authors (M.T.) and her group introduced a type of market model called potentials of unbalanced complex kinetics (PUCK), wherein the market price is described by a random walker in a temporally deforming potential force whose center is given by the trace of the walker [14–17]. This model has quite different statistical properties from the case of the fixed potential function, i.e., the Uhlenbeck-Ornstein process [18]. Moreover, the continuum

limit of PUCK model is shown to be equivalent to the Langevin equation with time-dependent coefficients [19].

From the viewpoint of this model with a quadratic potential function, market states are categorized into five conditions characterized by the potential function:

(1) A pure random-walk state, which is given by the case of no potential force. In mathematical finance, this condition is assumed to be the generic property of the price fluctuation of a financial market.

(2) A stable state, which is described by an attractive potential force. In this case, the market price tends to be attracted to the center of potential function. Corresponding Hurst exponent, which characterizes the abnormal diffusion, is smaller than 0.5 in short time scale and it converges to 0.5 in large time scale. Peinke and co-workers showed the existence of similar kind of attractive potential in foreign exchange market [20]; however, it should be noted that their analysis is based on the fixed potential function of Uhlenbeck-Ornstein type. Ausloos and Ivanova applied the same method and obtained similar results for the stock index data [21]. This model is also well known in the study of the “mean-reverting behavior” such as the electricity market price [22,23]. In these cases, the Hurst exponent almost converges to 0 in large time scale. The PUCK with an attractive potential function becomes an Uhlenbeck-Ornstein process in the special case that the center of the potential function is fixed.

(3) An unstable state, which is described by a repulsive potential force. In this case, the market price is repelled from the center of potential function. The corresponding Hurst exponent is larger than 0.5, in short time scale, it also converges to 0.5 in large time scale.

(4) A nonstationary state, which is characterized by a too-strong attractive force causing a divergence with the oscillation of price [24].

(5) A nonstationary state, which is characterized by a strong repulsive force causing nearly monotonic price changes as a result.

The PUCK model is known to satisfy basic market statistics such as the power-law distribution of price changes

*watanabe@smp.dis.titech.ac.jp

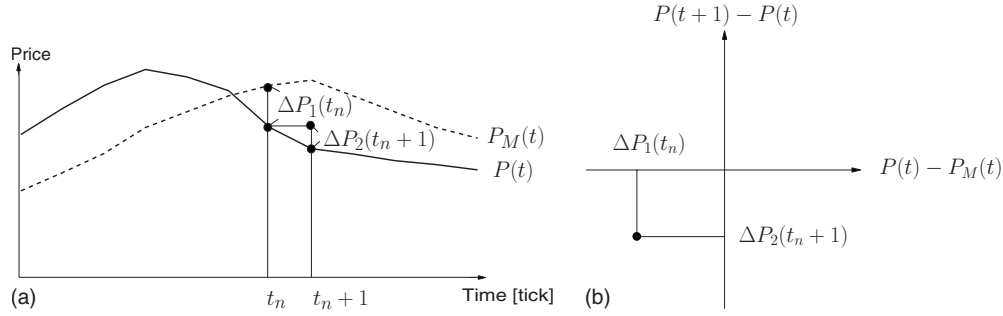


FIG. 1. Schematic diagram of the PUCK model. For given market time series, we calculate $P(t+1) - P(t)$ and $P(t) - P_M(t)$ as shown in the (a). The plot in (b) is proportional to the derivative of the potential function $-\frac{d}{dp}U(p, t)$.

[25–28], rapid decay of the autocorrelation of price changes [13], long correlation of the square of price changes [13], and abnormal diffusion properties [29] in a short time scale [30]. It has been clarified that the market potential force is closely related to the mass behavior of dealers, especially, the trend-following behavior [31,32]. Moreover, the Nobel prize laureated market model—the autoregressive conditional heteroskedasticity model—is derived in a very special limit case, where a higher-order asymmetric potential force appears with randomly chosen signs at each time step [33].

In this paper, we reformulate the data analysis method of PUCK taking into account the higher-order potential functions, and we focus our attention on finding and describing the price changes before and during financial bubbles and crashes. The data we analyze here, as examples, are the tick-by-tick data of dollar-yen exchange rates, which showed the largest rate change in 1998 and euro-yen exchange rates, which includes the recent financial crisis of 2008.

II. PUCK MODEL

The PUCK model is represented by the following set of equations:

$$P(t+1) - P(t) = -\frac{d}{dp}U(p, t)|_{p=P(t)-P_M(t)} + f(t), \quad (1)$$

$$P_M(t) = \frac{1}{M} \sum_{k=0}^{M-1} P(t-k). \quad (2)$$

Here, $P(t)$ is the noise-reduced market price at the t th tick obtained by applying the optimal moving average [34], $f(t)$ is the random noise typically a Gaussian white noise, $U(p, t)$ is the potential function, which is approximated by the following Taylor expansion form with time-dependent coefficients $b_k(t)$:

$$U(p, t) = \sum_{k=1}^{\infty} \frac{b_k(t)}{k+1} p^{k+1}. \quad (3)$$

Here, we do not include the term with $k=0$ in this expansion as such a term gives the same contribution as $f(t)$ in Eq. (1). $P_M(t)$ is the average of the past price changes with size M ticks, and it is assumed that this point gives the center of the potential function that moves with the random-walker’s footprint (Fig. 1). For the dollar-yen market, a typical value of

optimal M is smaller than ten. Additional information about the meaning of the optimal moving average M dependence of the PUCK analysis are explained in Appendixes A and B.

In Fig. 2, we show typical examples of potential functions observed in the dollar-yen market for given 2000 data points. Here, the mean interval of tick is about 15 s in both cases. The market fluctuations of Figs. 2(a) and 2(d) look very different intuitively; however, the square of the market price fluctuations in unit time called the volatility takes about the same value in both cases. More precisely, in Fig. 2(b), we can intuitively recognize that the market price $P(t)$ fluctuates around the averaged past price $P_M(t)$. So the market price does not fluctuate largely in long time scale. On the contrary, in Fig. 2(e), the market price separates from $P_M(t)$. The large scale price fluctuation of Fig. 2(d) is apparently larger than the case of Fig. 2(a) even microscopic volatilities take almost the same volatility. So we can recognize that there is instability of the market price, which we cannot quantify by the volatility.

By applying the PUCK model, we can clearly observe the difference in the quadratic term of the potential function, as shown in Figs. 2(c) and 2(f). In the case of Fig. 2(c), the value of $b_1(t)$ is positive and the market fluctuation is stable, while in the case of Fig. 2(f) the value of $b_1(t)$ is negative and market fluctuation is unstable. In both cases, there are abnormal diffusion properties in short time scale, as shown in Fig. 2(g) [24]. In the case of attractive potential force, it is slower than the normal diffusion, i.e., the Hurst exponent is smaller than 0.5 [● in Fig. 2(g)]. In the case of repulsive potential force, it is faster than the normal diffusion law, i.e., the Hurst exponent is larger than 0.5 [▲ in Fig. 2(g)]. However, in both cases, the long time behavior follows the normal diffusion property, i.e., the Hurst exponent is equal to 0.5 [dotted lines in Fig. 2(g)].

From the viewpoint of the agent model, the unstable potential force of market is known to be produced by dealer’s action of trend follow, which is a kind of herding behavior, and the stable potential force is caused by contrarians who follow mean-reverting behavior in which “mean” is given by the moving average $P_M(t)$. In this case, the market potential is strongly related to the majority strategy of dealers [31,32,35]. Especially in the case of ordinary mean-reverting model as mentioned in the introduction, the mean usually takes a constant value, namely, the model corresponds to the PUCK model in the limit of very large value of M in Eq. (2).

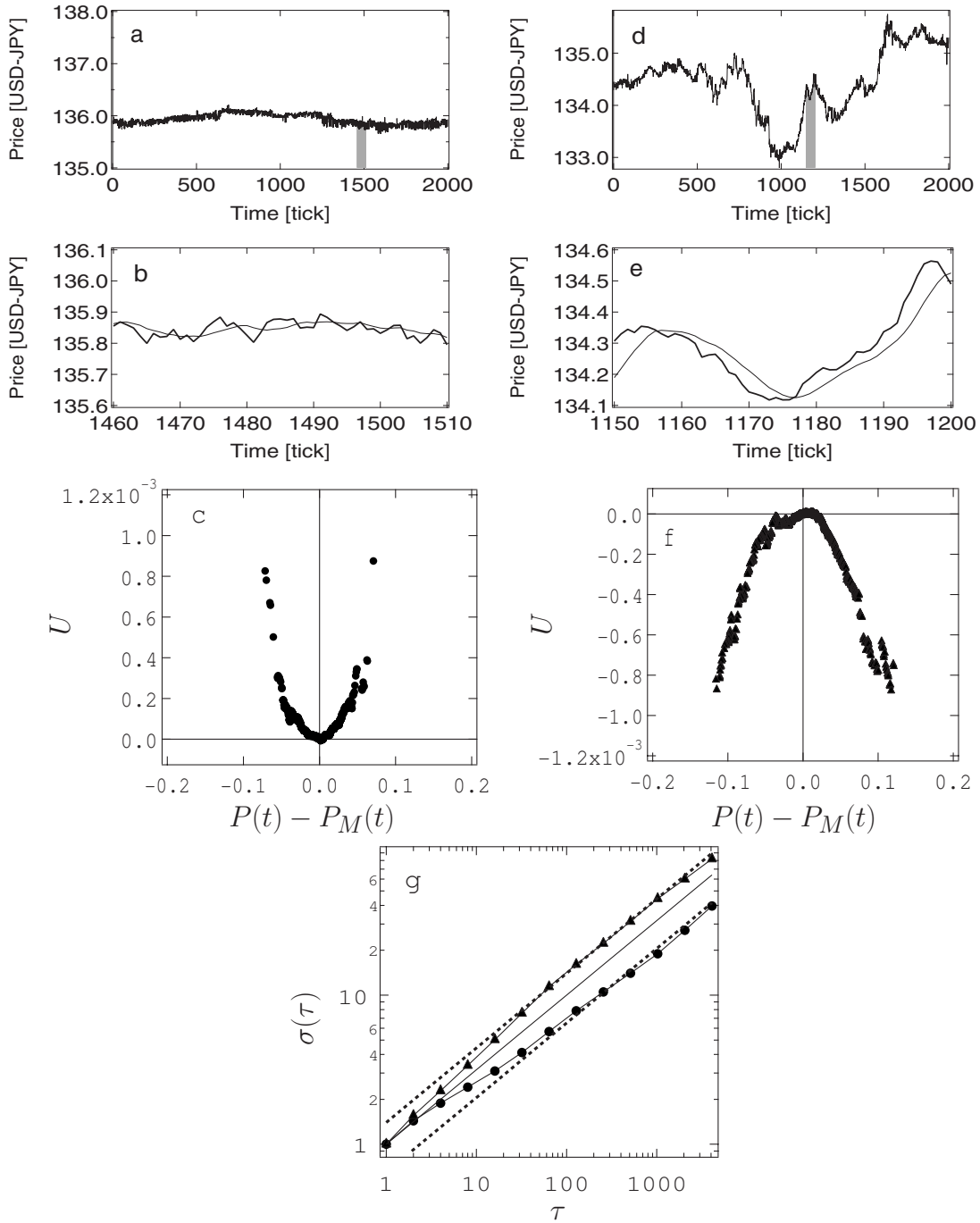


FIG. 2. Examples of estimated potential functions. For given dollar-yen rates, (a) and (d), the relations between $P(t)$ (heavy line) and $P_M(t)$ (thin line) are observed, as shown in (b) and (e) [enlarged view of gray areas of (a) and (d)], respectively. The potential functions [(c) and (f)] are estimated by integrating the plots of the diagram of Fig. 1(b). In (g), we show the diffusion of market price, $\sigma(\tau) = \sqrt{[P(t) - P(t-\tau)]^2}$ in the cases of (a) (●), (d) (▲), and pure random walk (line).

It is found that these quadratic potential functions can generally be found in normal states of financial markets; however, in particular periods, when prices move rather monotonically we can observe a type of nonquadratic potential functions, such as a cubic function, as shown later.

In order to describe such higher-order potential functions correctly, we take into account a higher-order term in the potential model as follows:

$$U(p,t) = \frac{b_1(t)}{2} p^2 + \frac{b_\gamma}{\gamma+1} p^{\gamma+1}. \tag{4}$$

When the market potential function is described by a cubic function ($\gamma=2$) with a local minimum point, there are obviously two states for the random walker, as shown schematically in Fig. 3. The first state is the trapped state that is practically the same as the case of a random walk in a stable

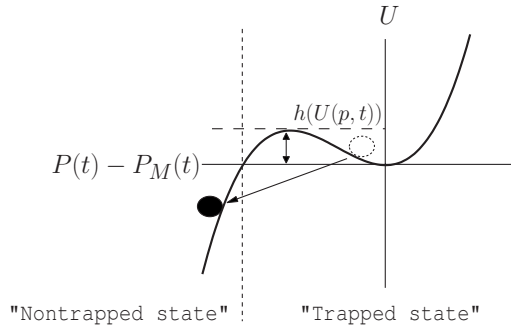


FIG. 3. Schematic diagram of the transition of price changes from a stable trapped state to a highly unstable nontrapped state.

quadratic potential function; however, in this state, there is an asymmetric price behavior, as shown in the trapped state of Fig. 4, which is created by a numerical simulation with a cubic potential model (in the case of a negative b_1 and a

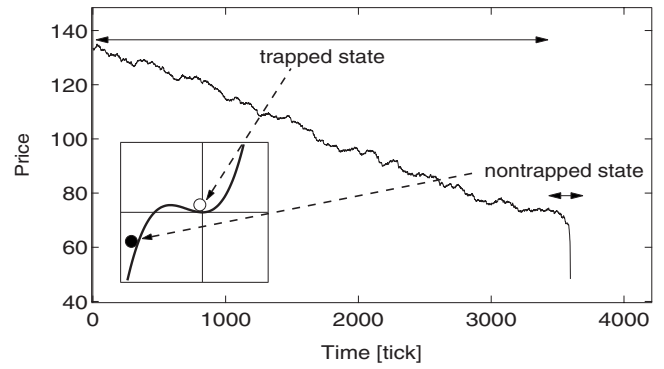


FIG. 4. A result of numerical simulation by using Eq. (1) with a cubic potential function [$\gamma=2$, $b_1=0.2$, $b_2=0.5$, and $M=5$ in Eq. (4)]. In this simulation, we use a Gaussian random number with the mean value 0 and the standard deviation $\eta=0.2$ for $f(t)$. In the subwindow of this figure, we show the cubic potential used in this simulation.

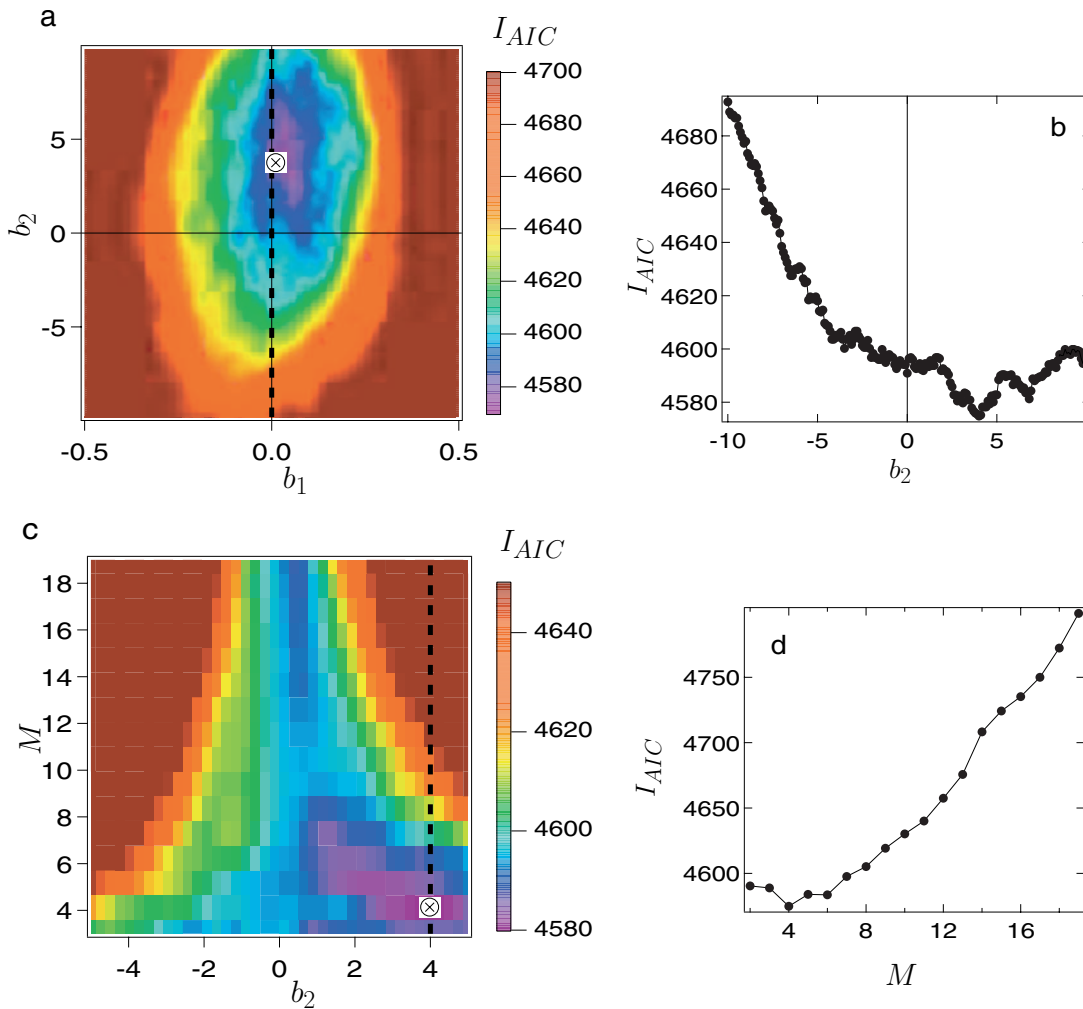


FIG. 5. (Color) The values of AIC in the parameter space. We search the optimal combination of parameters for the period b in Fig. 6. We show the figures of b_1 vs b_2 in the case of optimal $M=4$ (a), the cross section of dotted line ($b_1=0.0$ and $M=4$) of (a) [(b)], M vs b_2 in the case of $b_1=0.0$ (c), and the cross section of dotted line ($b_1=0.0$ and $b_2=4.0$) of (c) [(d)]. In these contour plots, we color the area by the amount of AIC. The color scales of AIC value are shown in the right hands of each figure. The optimal parameters are given by the set of parameters, which make the AIC value minimum are shown by \otimes .

positive b_2). Even in the trapped state, curvature of a cubic potential is not symmetric and the random walker takes different amount of force between $p > 0$ and $p < 0$. As a result, the market price shows a linear trend. This kind of market trend is observable in real market price changes, as shown later.

For a given cubic potential function, there is a finite possibility that the walker goes over the potential barrier. The second state is the nontrapped state, wherein the walker goes down the potential slope indefinitely following a double-exponential growth [36] or even the finite-time divergence in the continuum limit. In particular, we can expect a sudden transition of the movement of prices from a stable state to a highly unstable state even when the market potential function is invariant (the nontrapped state of Fig. 4). In the case of a positive b_1 and a negative b_2 , price transits from an uptrend (trapped state) to a sharp double-exponential increase (nontrapped state). Unless considering a higher-order potential term, the direction of slow trend (trapped state) and the sharp change (nontrapped state) is the same.

We observed transition times from an ordinary market trend to an extraordinary one by numerical simulation, the average time increases exponentially for higher potential barrier $h[U(p, t)]$, as expected from the Arrhenius-Kramers formula for random walker in a potential function [37]. From these results, the cubic potential is expected to describe both usual market trends and extraordinary market states such as financial bubbles and crashes.

Bouchaud and Cont proposed a similar idea of nonlinear Langevin equation for modeling stock market crashes [38]. They assume that the variation in the market price change is described by a Langevin model with a cubic velocity potential. However, there is a big difference between their model and the PUCK model. In the formulation of PUCK model, the center of the potential force is given by the moving average and the potential function is always shifting with the motion of the moving average. Also they did not consider the deformation of potential function.

III. ESTIMATION OF OPTIMAL POTENTIAL FUNCTIONS

For estimating the optimal potential function from real data, we need to consider the meaning of probability distribution of the independent random variable $f(t)$ in Eq. (1). From a skeptical viewpoint about the existence of the potential forces, one might think that any price movement can be fully described by only the random noise term $f(t)$, assuming that $f(t)$ takes extremely asymmetric values repeatedly by chance. This case is theoretically realizable; however, the probability of the occurrence of the whole event, which is estimated by the products of probability density of $f(t)$, becomes negligibly small for the cases of bubbles or crashes. This is confirmed systematically in the following manner.

For the given symmetric probability distribution of $f(t)$, $w[f(t)]$, we can calculate the probability of the occurrence of any time series by assuming that the process is governed by Eq. (1) with the potential function given by Eq. (4), and the parameters of the model are constants, namely, $b_1(t) = b_1, b_\gamma(t) = b_\gamma$, in the period from $t = n - N + 1$ to n . The prob-

ability of the occurrence or the likelihood of a given market price time series $\{P(n), P(n-1), \dots, P(n-N+1)\}$ is calculated by the following equation:

$$l(b_1, \gamma, b_\gamma, M) = \prod_{t=n-N+1}^n w[f(t)], \quad (5)$$

where each value of $f(t)$ is determined from Eq. (1) with Eq. (4). As for the functional form of the probability density of $f(t)$, we apply the Gaussian distribution with zero mean.

In statistics, this type of maximum-likelihood method is very popular, and the method of choosing the optimum number of parameters has already been established. In general, a model with more parameters has a greater tendency to receive a higher value of likelihood. In order to solve an overfitting problem and to evaluate which of the two models with different number of parameters is better, we should not use the likelihood itself but apply the information criterion called Akaike information criterion (AIC) that is composed of the logarithm of likelihood and the term of penalty, which depends on the number of parameters k [39],

$$I_{AIC} = -2 \ln l(b_1, \gamma, b_\gamma, M) + 2k. \quad (6)$$

We can determine the most appropriate parameter values of the potential function systematically by searching the smallest value of the AIC.

We compare the value of AIC for different values of k . The case of $k=0$ corresponds to a pure random-walk model, that is, $M=1$ and $U(p, t)=0$ in Eq. (1). The basic PUCK model belongs to the case of $k=2$, as there are two parameters M the moving average size and $b_1(t)$ the coefficient of the quadratic potential term. The cubic potential is introduced in the case of $k=2$ or 3, in which a higher-order potential term's coefficient $b_\gamma(t)$ is included as a new parameter. In the case of $k=2$ (only cubic term) or 3 (both quadratic and cubic terms), we consider all terms up to the fourth order of potential function. For each case of k , we find the combination of parameters, which makes the AIC minimum, as typically shown in Fig. 5 that is applied for the period (b) in Fig. 6.

In the contour plots of Figs. 5(a) and 5(c), we show the values of AIC of each parameter sets, as shown by the color scale of right sides of each figure. In Fig. 5(a), we show the values of AIC in the parameter sets of b_2 and b_1 in the case of $M=4$. We can get a minimum AIC value when the parameters are $b_2=4.0, b_1=0.0$, and $M=4$ (\otimes in this figure). Observing the cross-sectional diagram, as shown by the dotted line in Fig. 5(a) ($b_1=0.0$ and $M=4$), we can observe the minimum point of AIC [Fig. 5(b)]. In Fig. 5(c), we show the contour plot of AIC between b_2 and M in the case of $b_1=0.0$. From this figure and its cross-sectional diagram in the cases of $b_1=0.0$ and $b_2=4.0$, as shown in Fig. 5(d), the value of AIC becomes minimum when the value of $M=4$. From these results, we may say that the cubic potential is most appropriate to describe the market price change in Fig. 6 (2b). As mentioned above, we search the optimal model to minimize the value of AIC.

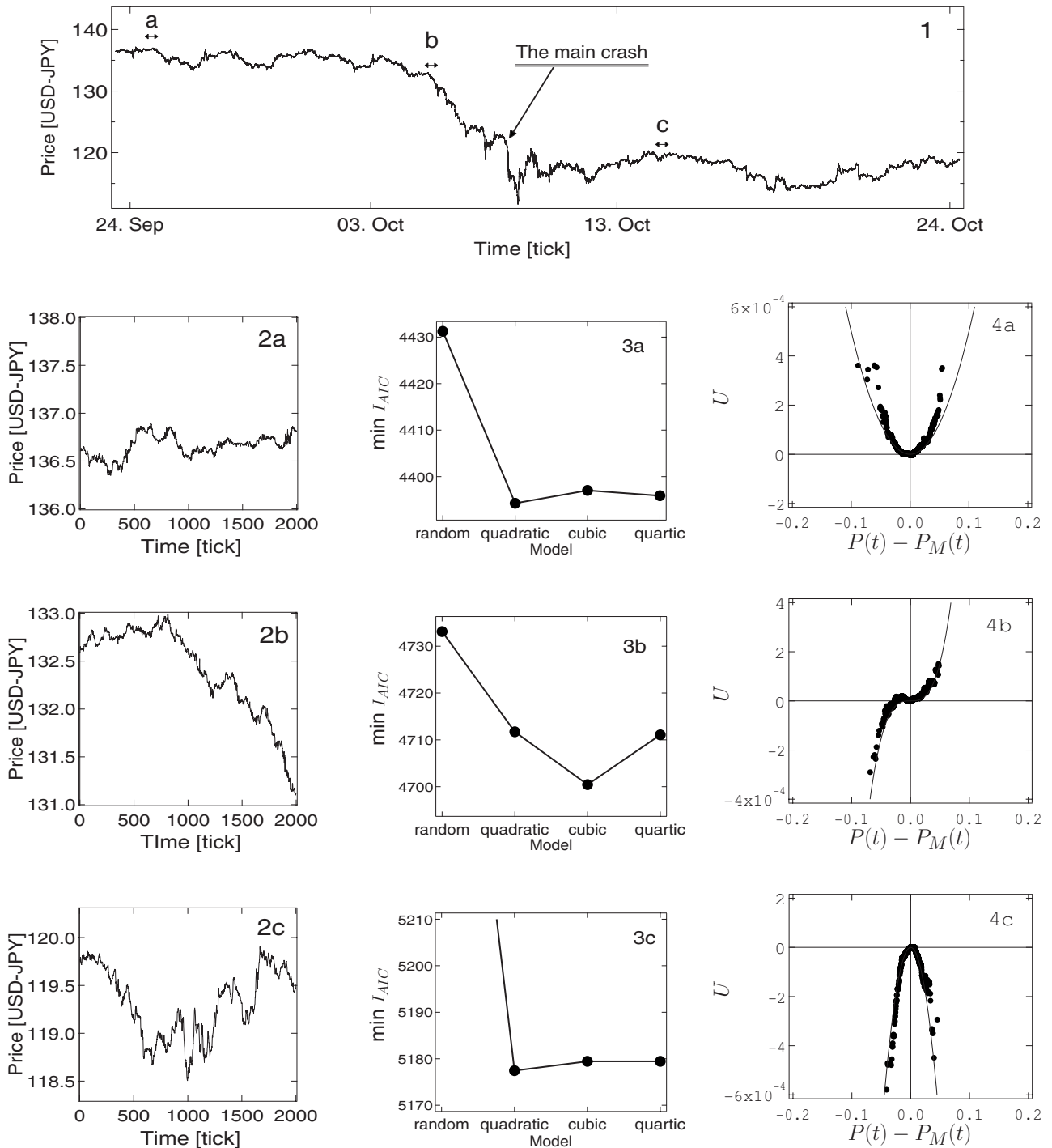


FIG. 6. Estimated optimal potential forms by the minimum information criterion procedure in the dollar-yen exchange rates of 1998 (1). (2) Time series of market price in period a, b, and c is shown. (3) The minimum AIC values, $\min I_{AIC}$, in the cases of pure random-walk model (random), the quadratic potential model (quadratic), the cubic potential model (cubic) and the quartic potential model (quartic). (4) Directly observed potential functions (●) and the optimal potential forms applying the AIC procedure with normal distribution to the term of $f(t)$ (line, window size $N=2000$).

Here, we observe two examples of our analysis applied to financial markets. The first example is dollar-yen exchange rates from September 23rd to October 26th in 1998 (as shown in Figs. 6 (1)), during this period the dollar-yen market showed historically the largest fluctuations. In Fig. 6 (3a–3c), we show a directly observed potential function from the

data in four periods, which are shown in Fig. 6 (2a–2c) with each window size $N=2000$ ticks. Additional information about N dependence of the PUCK analysis is explained in Appendix C. In Fig. 6 (4a–4c), we plot the minimum AIC values in the cases of pure random-walk model (random), the quadratic potential model (quadratic), the cubic potential

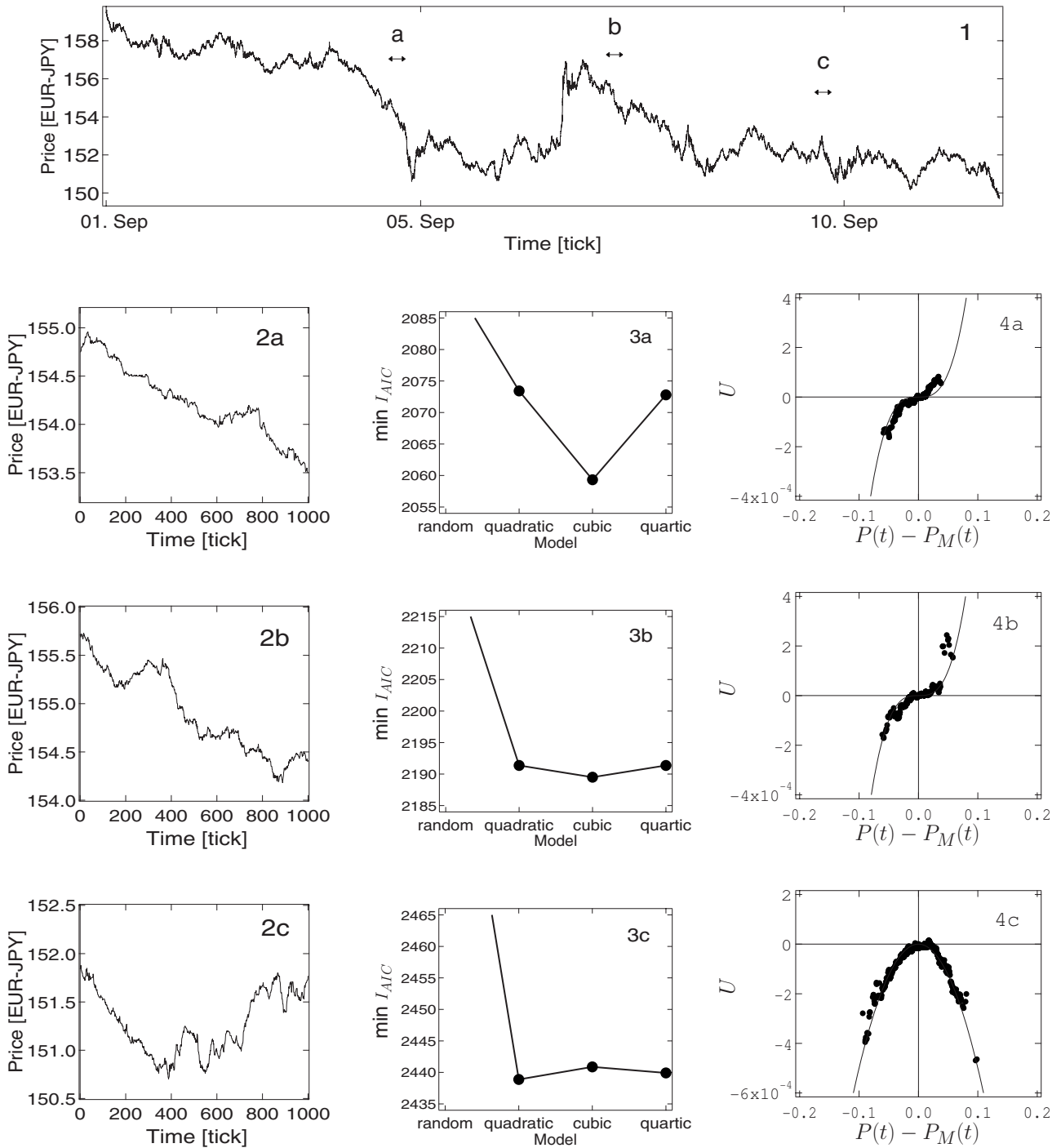


FIG. 7. Estimated optimal potential forms by the minimum information criterion procedure in the euro-yen exchange rates in September of 2008 (1). (2) Time series of market price in period a, b, and c is shown. (3) The minimum AIC values, $\min I_{AIC}$, in the cases of pure random-walk model (random), the quadratic potential model (quadratic), the cubic potential model (cubic), and the quartic potential model (quartic). (4) Directly observed potential functions (●) and the optimal potential forms applying the AIC procedure with normal distribution to the term of $f(t)$ (line, window size $N=1000$).

model (cubic), and the quartic potential model (quartic). From these figures, we can estimate the optimal potential form to describe the market price changes.

In the period denoted as “a” in Fig. 6 (1), the market price fluctuates rather stably, as shown in Fig. 6 (2a). In this case, the simple random-walk model with $k=0$ is the worst model

in view of AIC and the higher-order models are slightly behind the parabolic potential function with $k=2$ [Fig. 6 (3a)]. From these results, the most likely potential function is given by the quadratic function shown in the Fig. 6 (4a).

In period “b” we can clearly find a sharp drop in the latter half of Fig. 6 (2b), and the cubic potential model becomes

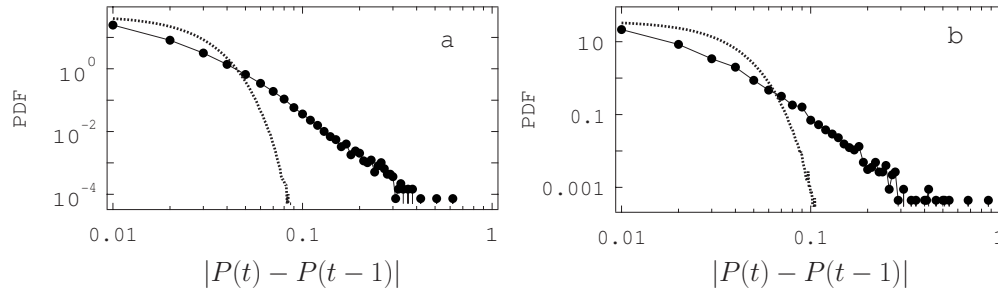


FIG. 8. Probability density function (PDF) of price changes $|P(t) - P(t - 1)|$ in the cases of dollar-yen exchange rates of 1998 (a) and euro-yen exchange rates of 2008 (b). We apply these empirical distributions as the case of fat-tailed distribution $f(t)$. In either case, the dotted line shows the normal distribution with the same mean and variance.

most optimal, as shown Fig. 6 (3b). The resulting most optimal potential function is given in Fig. 6 (4b), which is a quadratic function with a shallow well [Fig. 6 (4b)]. Similarly, in period “c” the main crash was over; however, the market is quite turbulent as shown in Fig. 6 (2c). The best model in this case is given by the quadratic potential function [Figs. 3(c) and 6] and its shape is shown in Figs. 6 (4c).

In Fig. 7, we observe the other example of euro-yen exchange rates from September 1st to 10th of 2008, during this period euro-yen exchange rates largely fluctuated, which was just before the breakdown of Lehman Brothers, September 15th. In the period “a” in Fig. 7 (1), the exchange rates decrease rather monotonically as shown in Fig. 7 (2a). The AIC value takes the smallest value by a cubic potential model, as demonstrated by Fig. 7 (3a), and the resulting best-estimated cubic potential function is given in Fig. 7 (4a). For the rest of cases of periods “b” and “c,” the potential functions are also estimated in the same way.

For further check of the method of information criterion, we also apply another information criterion called the Bayesian information criterion (BIC) [40]. Compared with AIC given by Eq. (6), this criterion modifies the penalty function with respect to the number of parameter k as a function of the number of data points N , as follows:

$$I_{BIC} = -2 \ln l(b_1, \gamma, b_\gamma, M) + k \ln(N). \quad (7)$$

We also take into account the effect of distribution function of $f(t)$ other than the normal distribution. For this purpose, we apply the empirically estimated price change distributions, as shown in Figs. 8(a) and 8(b) for dollar-yen and

euro-yen markets, which have fat tails approximated by power laws. Namely, we compare the results of optimal potential parameters with four types of analyses, i.e., AIC with the normal distributions of $f(t)$, BIC with the normal distribution, AIC with the fat-tailed distribution, and BIC with the fat-tail distribution.

In Tables I and II, the values of estimated optimal parameters of Figs. 6 and 7 are compared in each combinations of the information criteria and the distribution of $f(t)$. In any combinations and periods, we can get similar results of optimal parameter sets. As shown here, all major results mentioned in this paper are confirmed to be independent of the methods of analyses.

These results imply that the PUCK model with quadratic and cubic potential functions are suitable for describing these foreign exchange markets. Especially in the cases when cubic potential appears, the market price tends to move in the direction that the potential function declines. In Appendix E, we show more detail information about the statistical properties of market price changes when a cubic potential appears.

IV. DISCUSSION

In this paper, we presented a higher-order potential model suitable for the analysis of the market forces observed in financial bubbles or crashes. In order to show the statistical significance of the existence of higher-order potential functions, we applied the information criteria AIC and BIC. In the given examples, clear cubic potential functions were detected in the periods including crashes.

Similar higher-order potential functions can be confirmed in many other examples before and during bubbles and

TABLE I. Estimated values of b_1 , b_2 , and M in the three periods in Fig. 6. In this table, we show the optimal parameters by using the AIC with normal distribution, the BIC with normal distribution, AIC with fat-tail distribution, and BIC with fat-tail distribution.

Period	AIC with normal dist.			BIC with normal dist.			AIC with fat-tail dist.			BIC with fat-tail dist.		
	b_1	b_2	M	b_1	b_2	M	b_1	b_2	M	b_1	b_2	M
a	0.1	0.0	9	0.1	0.0	9	0.1	0.0	9	0.1	0.0	9
b	0.0	4.0	4	0.0	4.0	4	0.0	4.0	4	0.0	4.0	4
c	-0.6	0.0	2	-0.6	0.0	2	-0.6	0.0	2	-0.6	0.0	2

TABLE II. Estimated values of b_1 , b_2 , and M in the three periods in Fig. 7. In this table, we show the optimal parameters by using the AIC with normal distribution, the BIC with normal distribution, AIC with fat-tail distribution, and BIC with fat-tail distribution.

Period	AIC with normal dist.			BIC with normal dist.			AIC with fat-tail dist.			BIC with fat-tail dist.		
	b_1	b_2	M	b_1	b_2	M	b_1	b_2	M	b_1	b_2	M
a	0.0	2.3	8	0.0	2.3	8	0.0	4.1	2	0.0	4.1	2
b	0.0	2.4	6	0.0	2.4	6	0.0	2.4	3	0.0	2.4	3
c	-0.1	0.0	9	-0.1	0.0	9	-0.1	0.0	6	-0.1	0.0	6

crashes of financial markets. However, we cannot say that we can always observe the cubic potential function before the financial crisis.

Application of the method we developed in this paper is not limited to financial market data. As known from the formulation, this method is applicable to any time series, showing random-walk-like behaviors. For examples, medical data from patients, machine condition data in factories, environmental, and climate data are promising candidates for applying this method for early detection of nonstationary symptoms.

ACKNOWLEDGMENTS

This work is partly supported by Research Foundations of the Japan Society for the Promotion of Science for Young Scientists (K.W.) and Japan Society for the Promotion of Science, Grant-in-Aid for Scientific Research No. 16540346 (M.T.).

APPENDIX A: OPTIMAL MOVING AVERAGE PROCEDURE

In the PUCK analysis, we apply the optimal moving average as a pretreatment to given raw data $P_r(t)$ when the data show nonzero autocorrelation of price difference $\Delta P(t) = P(t) - P(t-1)$ or if outliers are included. An example of raw data's autocorrelation $C(T) = \langle \Delta P(t+T)\Delta P(t) \rangle / \langle \Delta P(t)^2 \rangle$ is shown in Fig. 9. There is a strong negative autocorrelation at 1 tick, which represents zig-zag behaviors in the time series of raw data, the dotted line in Fig. 10(a). Without the pretreatment, we observe a strong attractive potential function, as shown in Fig. 10(b) by the PUCK analysis. This attractive potential is generally very strong; however, this potential works only for zig-zag behaviors of market price in the very short time scale. In order to observe potential functions for

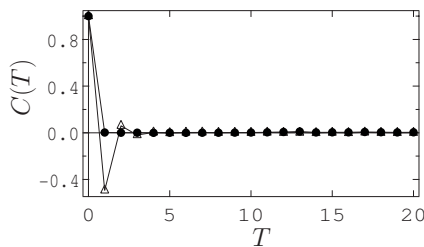


FIG. 9. Autocorrelation of raw price difference $P_r(t) - P_r(t)$ (Δ) and the noise term $\epsilon(t)$ (\bullet).

longer time scale, we need to smooth out such short-time fluctuation.

For the elimination of such short scale correlated fluctuation, we introduce the optimal moving average given by the following equations [34]:

$$P(t) = \sum_{j=1}^s \omega_j P_r(t-j), \quad (\text{A1})$$

$$P_r(t) = P(t) + \epsilon(t). \quad (\text{A2})$$

Here, $P(t)$ denotes the smoothed data, $\{\omega_j\}$ are the weights, which are determined by minimizing the square prediction variance $\langle \epsilon(t)^2 \rangle$ through solving the following Yule-Walker equation, which is familiar in the field of time series analysis based on autoregressive models. For the tick data of foreign exchange markets, $\{\omega_j\}$ is negligibly small for $j > 15$,

$$\langle \epsilon(t)^2 \rangle = \left\langle \left[P_r(t) - \sum_{j=1}^s \omega_j P_r(t-j) \right]^2 \right\rangle, \quad (\text{A3})$$

$$\begin{bmatrix} \Gamma_0 & \Gamma_1 & \cdots & \Gamma_{s-1} \\ \Gamma_1 & \Gamma_0 & \cdots & \Gamma_{s-2} \\ \vdots & \vdots & \ddots & \vdots \\ \Gamma_{s-1} & \Gamma_{s-2} & \cdots & \Gamma_0 \end{bmatrix} \begin{bmatrix} \omega_1 \\ \omega_2 \\ \vdots \\ \omega_s \end{bmatrix} = \begin{bmatrix} \Gamma_1 \\ \Gamma_2 \\ \vdots \\ \Gamma_s \end{bmatrix}. \quad (\text{A4})$$

Here, the autocovariance Γ_j is defined as

$$\Gamma_j = \langle [P_r(t) - \langle P_r(t) \rangle][P_r(t+j) - \langle P_r(t) \rangle] \rangle. \quad (\text{A5})$$

The thick line in Fig. 10(a) shows the smoothed market price and the autocorrelation of $\epsilon(t)$ almost vanishes, as shown in Fig. 9. The potential function estimated by the PUCK analysis for this smoothed price is shown in Fig. 10(c). This unstable quadratic potential function cannot be observed without the pretreatment.

It should be noted that there are cases that this pretreatment is not necessary when the autocorrelation of raw data almost vanishes like the deal data of electronic broking system (EBS), which is one of the world's largest computer trading systems in foreign exchange markets [41]. In such a case, the smoothed market price and the raw data are almost identical.

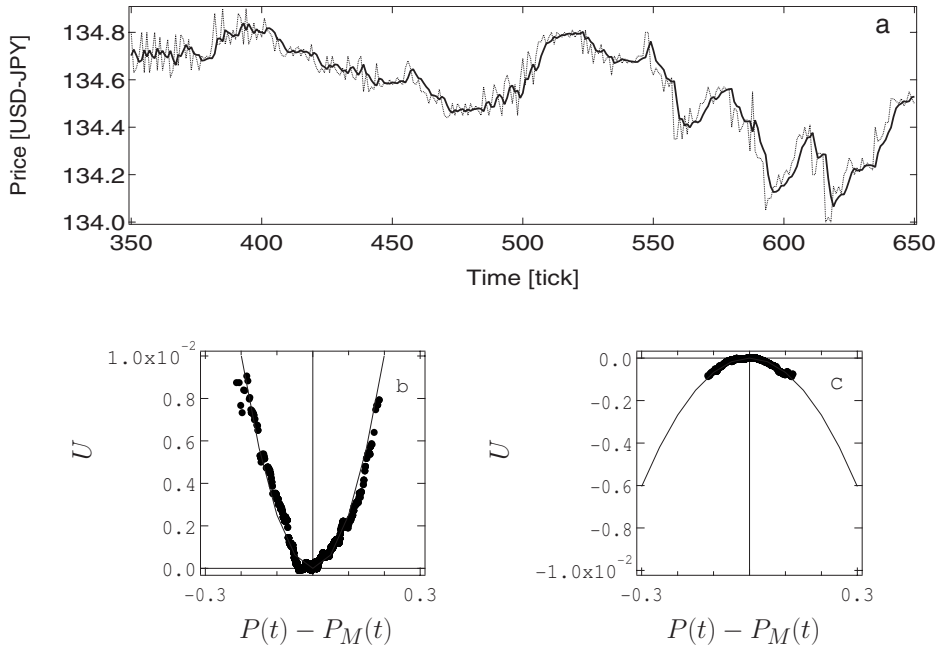


FIG. 10. Examples of optimal moving average procedure applied to a part of Fig. 2(d). In (a), we show the time series of raw market price $P_r(t)$ (dotted line) and the optimal moving average price $P(t)$ (heavy line) from 350 to 650 ticks of Fig. 2(d). We observe the potential functions (●) of 2000 ticks from the raw market price $P_r(t)$ (b) and from the optimal moving averaged price $P(t)$ (c). Due to the zig-zag fluctuation around the optimal moving average, the unstable potential (c) cannot be observed directly from the raw market price data.

APPENDIX B: M DEPENDENCE OF THE POTENTIAL FUNCTION

In PUCK analysis, we need to determine the value of moving average size M of $P_M(t)$, the center of the potential force. As seen from Fig. 11(a), the strength of potential force depends on the value of M . For the case of quadratic potential functions, it is known that the potential functions $U(p, t)$ in various values of M collapse into one potential function by multiplying $M-1$, as shown in Fig. 11(b) [14]. In such a case, the quadratic potential coefficient b_1 can be estimated nearly independent of M . In general case, however, this type of scaling relation does not hold and estimation of the best value of M is necessary.

APPENDIX C: N DEPENDENCE OF THE POTENTIAL FUNCTION

The potential function observed by the PUCK analysis generally depends on the observation window size N . In Fig. 12, we show examples of potential functions observed with different values of N . As indicated in these figures, we observe four window sizes $N=200$ ticks, $N=2000$ ticks,

$N=6000$ ticks, and $24\,000$ ticks. In Fig. 13, we show the difference of optimal AIC values between the cubic model and the other models ΔI_{AIC} . The value of ΔI_{AIC} represents probabilistic advantage of the cubic model to the other models. If ΔI_{AIC} is positive, the cubic model is not superior to the other models. We search the value of N , which makes ΔI_{AIC} smallest.

Figure 12 (2a) shows the case of $N=200$ ticks, which corresponds to about an hour in real time scale. We can observe a cubiclike potential function, however, scattering of data points is large and statistical significance is not high enough, i.e., ΔI_{AIC} is larger than other cases. In Fig. 12 (2b), the case of $N=2000$ ticks is shown. Here, we can clearly observe a cubic potential function with high statistical significance, as confirmed in Fig. 13. In the cases of Fig. 12 (2c and 2d) with $N=6000$ and $N=24\,000$ ticks, which correspond to about over a day or a week in real time scale, we observe an unstable quadratic potential function. For such large window sizes, we observe an averaged potential function, so that the potential function tends to be weaker and more symmetric. Actually in Fig. 13, the values of ΔI_{AIC} become large again. Therefore, we know that we can optimize the window size N as 2000 for this time series.

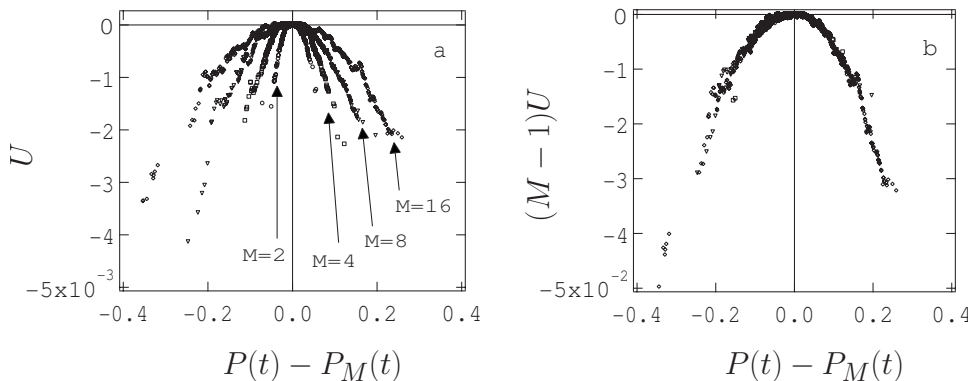


FIG. 11. Examples of M dependence of potential function in the case of Fig. 2(d). (a) The potential functions $U(p, t)$ in the cases of $M=2$ (○), 4 (□), 8 (▽), and 16 (◇). (b) The normalized potential functions $(M-1)U(p, t)$ in the cases of $M=2$ (○), 4 (□), 8 (▽), and 16 (◇). All cases collapse into a parabolic potential function indicating that $b_1(t)$ can be estimated from the curvature of (b) independent of M .

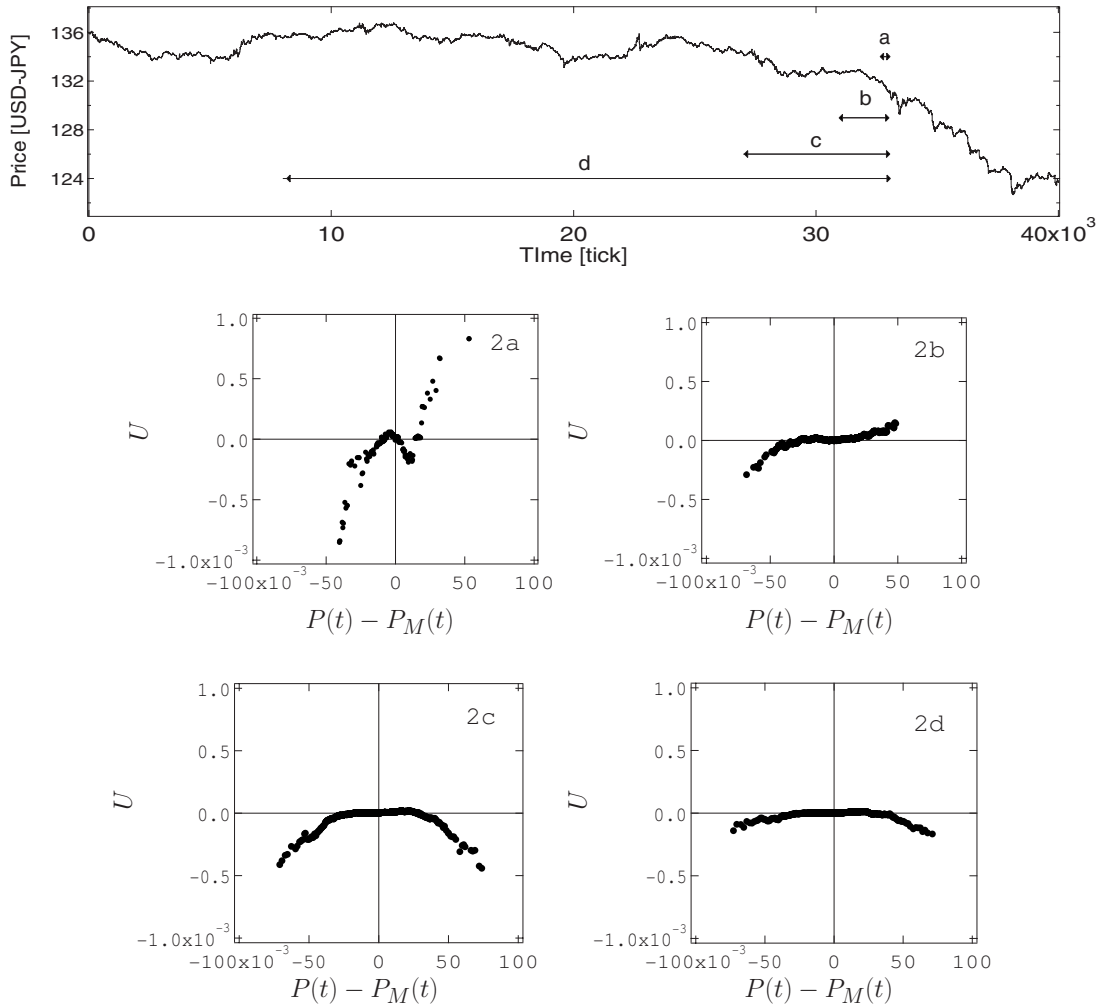


FIG. 12. Examples of N dependence of potential function. We show directly observed potential functions (●) from the data of 200 ticks [$b_1=0.1, b_2=8.3$, and $M=4$ in period (a)], 2000 ticks [$b_1=0.0, b_2=4.0$, and $M=4$ in period (b)], 6000 ticks [$b_1=0.1, b_2=0.8$, and $M=4$ in period (c)], and 24 000 ticks [$b_1=0.0, b_2=0.0$, and $M=4$ in period (d)].

APPENDIX D: TIME EVOLUTION OF POTENTIAL FUNCTION

Time evolution of quadratic potential function is known to be well approximated by the Ornstein-Uhlenbeck process. The PUCK model with this stochastic motion of $b_1(t)$ satisfies basic stylized facts such as the power-law distribution of price changes, rapid decay of the autocorrelation of price change, long correlation of volatility, and abnormal diffusion properties in a short time scale [30]. Moreover, the potential coefficient is strongly related to the mass behavior or strategy of market dealers. It is also important to observe how the parabolic potential changes to the cubic potential.

Here, we particularly focus on the transition process from the quadratic potential to the cubic one. In Table III, we calculate the transition probabilities that a stable quadratic potential $b_1 > 0$ changes to the cubic potential and an unstable quadratic potential changes to the cubic potential in the case of dollar-yen exchange rates in 1998. The transition probability is largest from an unstable quadratic potential. Transition from a cubic potential state is also analyzed and the results are summarized in the right hand of Table III. The

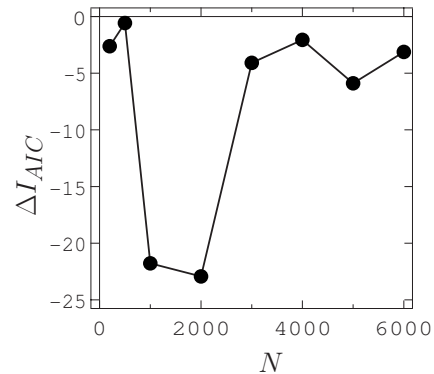


FIG. 13. Example of N dependence of $\Delta I_{AIC} = I_{AIC}^{opt}(\gamma=2) - I_{AIC}^{opt}(\gamma < 2)$ in the case of Fig. 12. At this point, $I_{AIC}^{opt}(\gamma=2)$ shows the optimal value of AIC of cubic model. $I_{AIC}^{opt}(\gamma=0)$ shows the optimal AIC of random walk. $I_{AIC}^{opt}(\gamma=1)$ shows the optimal AIC of quadratic model. We can evaluate probabilistic advantage of the cubic model by this value.

TABLE III. Transition probabilities from three states [a stable quadratic potential, a pure random walk (no potential), and an unstable quadratic potential] to a cubic potential state, and the transition probabilities from a cubic potential state to the three states in the case of dollar-yen exchange rates of 1998. The total number of samples is 693. We define the cubic potential as the cases in which $b_2 > 0$ (or $b_2 < 0$) continuously over 100 ticks.

Before	Transition probability		Transition probability	After
Stable quadratic	0.146		0.130	Stable quadratic
Pure random walk	0.333	⇒Cubic⇒	0.315	Pure random walk
Unstable quadratic	0.521		0.555	Unstable quadratic

transition probability is largest also to an unstable quadratic potential state.

APPENDIX E: STATISTICAL PROPERTIES OF MARKET PRICE CHANGES WHEN A CUBIC POTENTIAL APPEARS

By using the dollar-yen exchange rates of 1998 [Fig. 14(a)] and the euro-yen exchange rates of 2008 [Fig. 14(b)], we calculate the probability densities of price changes when cubic potential functions are observed. In Fig. 15, the probability density of price changes, $\Delta P(t, t-N) = P(t) - P(t-N)$ are plotted for the window size N under the condition that the cubic potential is detected in the same time interval $[t-N, t]$. The numbers of events we observed clear cubic potential functions are about 700 in the year 1998 and about 600 in the year 2008.

In the case that the coefficient of cubic potential function is negative $b_2(t) < 0$, the peak of the probability density of price change $p[\Delta P(t, t-N)]_{b_2(t) < 0}$ (line with ●) shifts to positive, and in the case $b_2 > 0$, the probability density $p[\Delta P(t, t-N)]_{b_2(t) > 0}$ (line with *) shifts to negative, as shown in Figs. 15(a) and 15(b). For comparison, the probability densities of price changes in the interval N ticks for

all data are plotted by the dotted lines with ○, which are almost symmetric in both cases. As the coefficient b_2 is estimated using the data in the interval $[t-N, t]$, these results show that the cubic potential and the net price change in the observation interval are strongly related.

Next, we check the correlation between the future market price change and the cubic potential function. We observe the price change at T ticks after t , $\Delta P(t+T, t) = P(t+T) - P(t)$, under the condition that a cubic potential function is detected in the time interval $[t-N, t]$. We count the following numbers of events. Let $S_{<}(+|T)$ be the number of events in which $\Delta P(t+T, t) > 0$ with $b_2(t) < 0$, $S_{<}(-|T)$ be the number

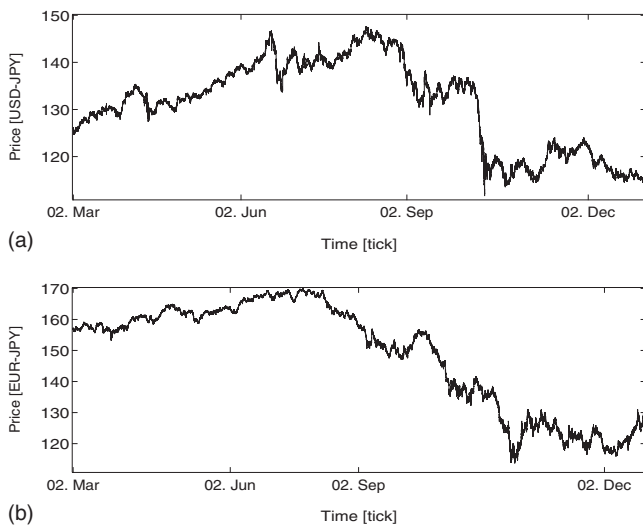


FIG. 14. Time series of dollar-yen exchange rates of 1998 (a) and the euro-yen exchange rates of 2008 (a) from March until the end of December. In each case, market prices tend to decline in the latter.

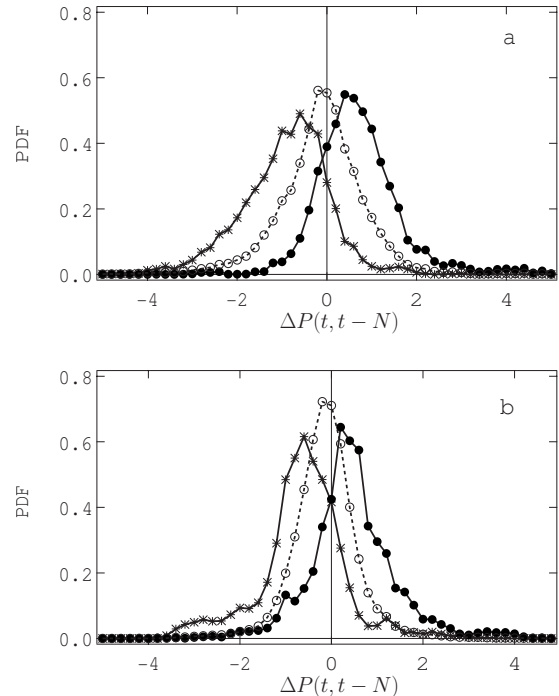


FIG. 15. Probability densities of three conditional market price changes in N ticks $p[\Delta P(t, t-N)]$ (dotted line with ○), $p[\Delta P(t, t-N)]_{b_2(t) > 0}$ (line with *), and $p[\Delta P(t, t-N)]_{b_2(t) < 0}$ (line with ●), in the cases of dollar-yen exchange rates of 1998 [window size $N=2000$ in (a)] and euro-yen exchange rates of 2008 [window size $N=1000$ in (b)]. In both cases, $p[\Delta P(t, t-N)]$ is almost symmetric around 0. However, in the cases of $p[\Delta P(t, t-N)]_{b_2(t) > 0}$ and $p[\Delta P(t, t-N)]_{b_2(t) < 0}$, average of $\Delta P(t, t-N)$ is clearly different from 0. The market prices fluctuate with a trend, which is given by the slope of the cubic potential function.

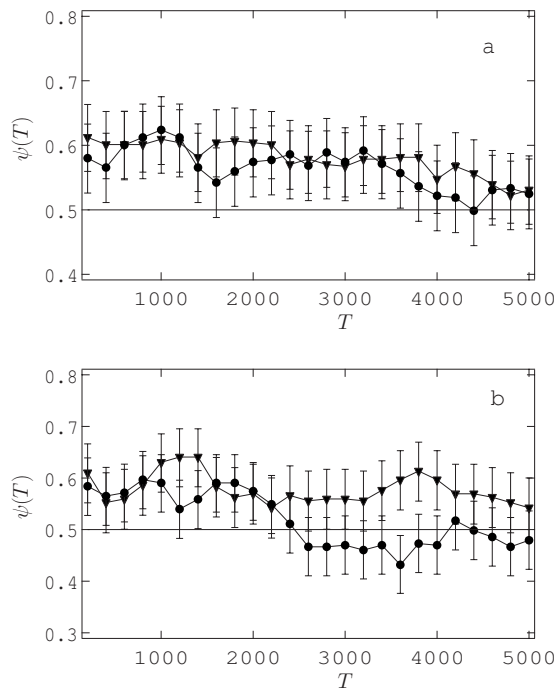


FIG. 16. The values of $\psi_{<}(T)$ (●) and $\psi_{>}(T)$ (▼), T ticks after a cubic potential function is continuously observed at 100 ticks in the cases of dollar-yen exchange rates of 1998 (a) and euro-yen exchange rates of 2008 (b). The error bars indicate the two-sided 95% confidence interval by assuming the binomial distribution of price up or down. In all cases, the values are significantly larger than 0.5, the value for a random walk, for $T < 2000$.

of events in which $\Delta P(t+T, t) < 0$ with $b_2(t) < 0$, $S_{>}(+|T)$ be the number of events in which $\Delta P(t+T, t) > 0$ with $b_2(t) > 0$, and $S_{>}(-|T)$ be the number of events in which $\Delta P(t+T, t) < 0$ with $b_2(t) > 0$. From these quantities, we calculate the probabilities that the direction of slope of cubic potential function agrees with the future price change $\psi_{<}(T)$ and $\psi_{>}(T)$, which are defined by the following equations:

$$\psi_{<}(T) = \frac{S_{<}(+|T)}{S_{<}(+|T) + S_{<}(-|T)}, \quad (\text{E1})$$

$$\psi_{>}(T) = \frac{S_{>}(-|T)}{S_{>}(+|T) + S_{>}(-|T)}. \quad (\text{E2})$$

The values of $\psi_{<}(T)$ (●) and $\psi_{>}(T)$ (▼) are plotted for various values of T in Fig. 16, in the cases of dollar-yen exchange rates of 1998 [Fig. 16(a)] and euro-yen exchange rates of 2008 [Fig. 16(b)]. In both exchange rates, there are large crashes of market price in the latter half of the year. The error bars denote the two-sided 95% confidence interval by assuming an independent binomial distribution of price up or down. In both cases, the values of $\psi_{<}(T)$ and $\psi_{>}(T)$ are significantly larger than 0.5, the value for pure random case, for T smaller than 2000 ticks, which corresponds to several hours in physical time. For a longer time scale, the random nature prevails in any case.

- [1] F. Lillo and R. N. Mantegna, *Eur. Phys. J. B* **15**, 603 (2000).
 [2] K. Watanabe, H. Takayasu, and M. Takayasu, *Physica A* **382**, 336 (2007a).
 [3] K. Watanabe, H. Takayasu, and M. Takayasu, *Physica A* **383**, 120 (2007b).
 [4] T. Mizuno, H. Takayasu, and M. Takayasu, *Physica A* **308**, 411 (2002).
 [5] A. Johansen and D. Sornette, *Physica A* **294**, 465 (2001).
 [6] D. Sornette and J. Andersen, *Int. J. Mod. Phys. C* **13**, 171 (2002).
 [7] N. Vandewalle, M. Ausloos, P. Boveroux, and A. Minguet, *Eur. Phys. J. B* **4**, 139 (1998).
 [8] N. Vandewalle, M. Ausloos, P. Boveroux, and A. Minguet, *Eur. Phys. J. B* **9**, 355 (1999).
 [9] D. Sornette, H. Takayasu, and W. X. Zhou, *Physica A* **325**, 492 (2003).
 [10] W. X. Zhou and D. Sornette, *Physica A* **361**, 297 (2006).
 [11] J.-P. Bouchaud and M. Potters, *Theory of Financial Risks* (Cambridge University Press, Cambridge, 2000).
 [12] L. Bachelier, *The Random Character of Stock Market Prices* (MIT, Cambridge, 1964).
 [13] R. Mantegna and H. E. Stanley, *An Introduction to Econophysics: Correlation and Complexity in Finance* (Cambridge University Press, Cambridge, 2000).
 [14] M. Takayasu, T. Mizuno, T. Ohnishi, and H. Takayasu, in *Practical Fruits of Econophysics*, edited by H. Takayasu (Springer-Verlag, Tokyo, 2005), p. 29.
 [15] M. Takayasu, T. Mizuno, and H. Takayasu, e-print arXiv:physics/0509020.
 [16] M. Takayasu, T. Mizuno, and H. Takayasu, *Physica A* **370**, 91 (2006).
 [17] V. Alfi, F. Coccetti, M. Marotta, L. Pietronero, and M. Takayasu, *Physica A* **370**, 30 (2006).
 [18] G. Uhlenbeck and L. Ornstein, *Phys. Rev.* **36**, 823 (1930).
 [19] M. Takayasu and H. Takayasu, *Prog. Theor. Phys.* **179**, 1 (2009).
 [20] R. Friedrich, J. Peinke, and C. Renner, *Phys. Rev. Lett.* **84**, 5224 (2000).
 [21] M. Ausloos and K. Ivanova, *Phys. Rev. E* **68**, 046122 (2003).
 [22] J. Perello, M. Montero, L. Palatella, I. Simonsen, and J. Masoliver, *J. Stat. Mech.: Theory Exp.* (2006) P11011.
 [23] H. Higgs and A. Worthington, *Energy Econ.* **30**, 3172 (2008).
 [24] T. Mizuno, M. Takayasu, and H. Takayasu, *Physica A* **382**, 187 (2007).
 [25] B. B. Mandelbrot, *Journal of Business* (University of Chicago Press, Chicago, 1963), Vol. 36, p. 394.
 [26] X. Gabaix, P. Gopikrishnan, V. Plerou, and H. E. Stanley, *Nature (London)* **423**, 267 (2003).
 [27] P. Gopikrishnan, M. Meyer, L. A. N. Amaral, and H. E. Stanley, *Eur. Phys. J. B* **3**, 139 (1998).

- [28] J. D. Farmer and F. Lillo, *Quant. Finance* **4**, C7 (2004).
- [29] V. Plerou, P. Gopikrishnan, L. A. Nunes Amaral, X. Gabaix, and H. E. Stanley, *Phys. Rev. E* **62**, R3023 (2000).
- [30] M. Takayasu, K. Watanabe, T. Mizuno, and H. Takayasu, in *New Approaches to the Analysis of Large-Scale Business and Economic Data*, edited by M. Takayasu, T. Watanabe, and H. Takayasu (Springer-Verlag, Berlin, in press).
- [31] K. Yamada, H. Takayasu, and M. Takayasu, *Eur. Phys. J. B* **63**, 529 (2008).
- [32] K. Yamada, H. Takayasu, T. Ito, and M. Takayasu, *Phys. Rev. E* **79**, 051120 (2009).
- [33] M. Takayasu, T. Mizuno, and H. Takayasu, *Physica A* **383**, 115 (2007).
- [34] T. Ohnishi, T. Mizuno, K. Aihara, M. Takayasu, and H. Takayasu, *Physica A* **344**, 207 (2004).
- [35] V. Alfi, M. Cristelli, L. Pietronero, and A. Zaccaria, *Eur. Phys. J. B* **67**, 385 (2009).
- [36] K. Watanabe, H. Takayasu, and M. Takayasu, *Prog. Theor. Phys.* **179**, 8 (2009).
- [37] P. Hanggi, P. Talkner, and M. Borkovec, *Rev. Mod. Phys.* **62**, 251 (1990).
- [38] J.-P. Bouchaud and R. Cont, *Eur. Phys. J. B* **6**, 543 (1998).
- [39] H. Akaike, in *Proceedings of the 2nd International Symposium on Information Theory*, edited by B. N. Petrov and F. Caski (Adademiai Kiado, Budapest, 1973), p. 267.
- [40] G. Schwarz, *Ann. Stat.* **6**, 461 (1978).
- [41] T. Ohnishi, H. Takayasu, T. Ito, Y. Hashimoto, T. Watanabe, and H. Takayasu, *J. Econ. Interact. Coord.* **3**, 99 (2008).